Formation and Decay Behaviors of Laser-Induced Transient Species from Pyrene Derivatives 2. Micellar Effects

Yoshihiro Mori,* Hiroyuki Shinoda, Taku Nakano, and Taiji Kitagawa

Department of Pharmaceutical Sciences, Toyama Medical and Pharmaceutical University, Sugitani, Toyama 9300194, Japan

Received: February 5, 2002; In Final Form: August 16, 2002

Micellar effects were investigated on the decay behaviors of several transient species such as triplet and cation radical that were produced by laser irradiation of three pyrene derivatives (sodium pyrenesulfonate (NaPS), tetrasodium pyrenetetrasulfonate (Na_4PS_4), and pyrenebutyric acid (HPB)). Those compounds were solubilized in Aerosol OT (AOT) reverse micellar solutions with different molar ratios of $[H_2O]/[AOT]$(W). The W-dependent decay curves of triplets from PS_4^{4-} and PS^- were analyzed with the kinetic model involving both the intra- and intermicellar triplet−triplet annihilations (TTA). As a result, the triplets were found to decay through two different TTA mechanisms: $T + T \rightarrow T + S0$ for PS_4^{4-} triplet and $T + T \rightarrow S1 + S0$ for PS^- triplet, respectively. It is shown that the PS_4^{4-} triplet is a useful probe for determination of the aggregation number per micelle. In the case of their cation radicals, the decay curves, in addition to the yields, were found to largely depend on W and atmospheric gases. The present results can be interpreted in terms of size and physicochemical properties of the water pool, location of the probe molecule in a micelle, and the nature of the cation radical formed. The dependence of the cation radical from PS^- is consistent with the two distinct locations model in which PS^- molecules are distributed into both water pool and palisade layer. On the other hand, two types of cation radicals, completely charge-separated and intramolecular charge-separated species, have been proposed to explain the observed decay curves of the cation radical from PS_4^{4-} in the water pool. Both the formation and the decay behavior of the latter cation radical were found to reflect the ionic environment of the water pool.

Introduction

Micellar systems are one of the model systems that have extensively been used to investigate the structural and dynamic properties of a restrictive environment. Various methods have been employed to probe and characterize their microscopic environments. Among them, the fluorescence method has remained potent even in very recent years, by which their size and microscopic properties (polarity, viscosity, chemical equilibrium) have been determined.[1−7] Fluorescence measurements are usually done by exciting a selected fluorescent molecule incorporated as the probe with a low-power laser. Many transient species other than the fluorescent one, for example, cation and anion radicals, are also available to probe the micellar systems. These transient species are produced using a high-power laser and detected with transient absorption spectroscopy. This method has the merit that one can simultaneously probe the microenvironment with multiple species with different chemical properties. For practical application of this method, however, several problems need to be solved. The following two problems are decisive: (1) spectral separation of each transient species involving excited singlets, triplets, solvated electrons, cation radicals, anion radicals, etc., produced under irradiation of a high power laser; (2) their decay mechanisms in the absence and presence of any quenchers added. In the preceding article, we demonstrated that these hurdles could be overcome using several different pyrene derivatives.[8] Here, we investigate the micellar effects on formation and decay behaviors of those transient species and discuss their availability to probe the microenvironment of micellar systems.

Laser-induced transient absorption spectroscopy, together with fluorescence measurements, has usefully been applied in the early stage to study micellar systems. We briefly review the results reported. Grätzel et al. observed transient absorption (TA) spectra of pyrenesulfonate (PS^-) and pyrenebutyric acid (HPB) both in aqueous solution and in reverse micellar solution.[9] These two pyrene derivatives generated cation radicals, as well as triplets, after laser irradiation. The spectra due to the cation radical of HPB were similar in aqueous and reverse micellar solutions, while that of PS^- was not detected in reverse micellar solution. They explained this difference on the basis of the location of the probe molecules and suggested an important role of the micellar Stern layer in the photoionization process. They also discussed the micellar effects on the triplet−triplet annihilation (TTA) process. Rothenberger et al. analyzed the decay curves of T−T absorption on the basis of the TTA mechanism and determined the probe distribution among the micelles and the kinetic parameters on the intramicellar TTA processes.[10] Gauduel et al. revealed in femtosecond range the fate of an electron ejected via photoionization of phenothiazine (PTH) located in the surfactant phase of AOT reverse micelle (AOT = sodium bis(2-ethylhexyl)sulfosuccinate).[11] The ejected electron was found to promptly be trapped in the water pool and then to be hydrated. The trapping efficiency of the excess electron in the water pool increased with the size of the water pool. Ghosh et al. found that the ionization potential of PTH was lowered in SDS micellar solution (SDS = sodium dodecyl sulfate) with picosecond flash photolysis.[12] Recently, Grand measured the decay of the photoinduced tetramethylbenzidine

10.1021/jp020333d CCC: $22.00
Published on Web 11/13/2002

cation radical in reverse micellar solution as a function of the sign of the interfacial charge and the size of the water pool.[13,14] From the results, he pointed out the important role of the bound water of the interface region. We also investigated the two-photon ionization process of NaPS in an AOT reverse micelle, resulting in the formation of cation radicals (zwitterions), anion radicals (dianions), and hydrated electrons.[15] The yield of cation radicals was found to decrease with the decrease in the size of the water pool, that is, the molar ratio of [water]/[AOT]. The anion radical formed via an electron attachment to PS^- was detected only in the largest water pool where more than two NaPS molecules could be dissolved in the same micelle.[16]

Experimental Section

Sample Preparation. AOT (Tokyo Kasei) was purified following the method previously reported.[17] Dodecylammonium propionate (DAP) was prepared by neutralization of dodecylamine solution with propionic acid.[18] The other surfactants (pentaethylene glycol mono *n*-dodecyl ether ($C_{12}E_5$; Nikko Chemicals) and sodium octanoate (Wako Pure Chemical)) and solvents (isooctane, cyclohexane, *n*-octane, *n*-octanol) commercially available were also used without further purification. Fluorescent probes (Na_4PS_4, NaPS, and HPB) were purchased from Molecular Probe and used as received. Doubly distilled deionized water was employed.

Reverse micellar solutions were prepared as follows: (1) AOT reverse micellar solution was prepared by dissolving and mixing a constant volume of water into 0.1 M AOT/isooctane solution. The molar ratio of $[H_2O]/[AOT]$ (W) varied from 10 to 50. (2) DAP reverse micellar solution was prepared by dissolving water into 0.08 M DAP/cyclohexane solution with $[H_2O]/[DAP] = 9$.[19] The solution becomes opaque below 33 °C, so the measurements of TA were carried out at 36 °C. (3) $C_{12}E_5$ reverse micellar solution was prepared by dissolving water into 0.073 M $C_{12}E_5$/*n*-octane solution with $[H_2O]/[C_{12}E_5] = 22$. The solution was very viscous and easily phase-separated. Therefore, the measurements of TA were carried out at about 38 °C immediately after the transparent and homogeneous solution was prepared. (4) A reverse micellar solution composed of sodium octanoate (50 mM) containing 0.95 M *n*-octanol as cosurfactant was prepared using isooctane as the solvent with $[H_2O]/[\text{sodium octanoate}] = 30$. The concentration of the probe molecule ([probe]) usually adjusted to $1-2 \times 10^{-4}$ M. The sample solution was deaerated via several freeze−pump−thaw cycles and then displaced by Ar, O_2, or N_2O gas.

Measurements of TA and Fluorescence and Kinetic Analysis of Decay Curves. The method for measuring laser-induced TA spectra and the decay behavior was described previously.[8] In this experiment, the third harmonics of a Nd:YAG laser (355 nm; Surelite II/Hoya-Continuum) was used for excitation of the sample solution. The fluorescence lifetime of NaPS in AOT reverse micelle was measured as a function of W with NAES-700F (Horiba). The observed decay curves were analyzed with a standard nonlinear least-squares fitting method.

Results

1. T−T Absorption and T−T Annihilation. The absorption maximum for T−T absorption in AOT reverse micellar solution appeared at 430, 420, and 420 nm for Na_4PS_4, NaPS, and HPB probes, respectively. These peaks were the same as those in water or aqueous ethanol solution. No significant changes in the yields of triplets were also observed. The T−T absorption spectra of NaPS and Na_4PS_4 in AOT micellar solution will be shown in later sections (Figures 3 and 8, respectively). Their decay curves, however, were found to greatly depend on W, of which the dependence changed from one probe to another.

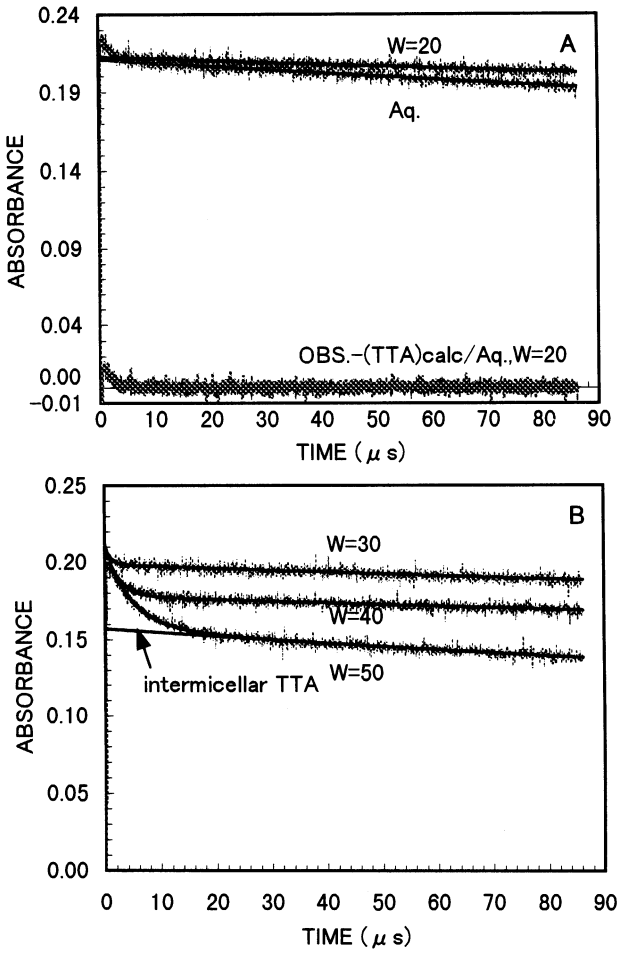

Figure 1. W dependence of decay curves for T−T absorption of PS_4^{4-} in AOT reverse micellar solution and the calculated curves by fitting to the intra- and intermicellar TTA kinetics. All of the decay curves were observed at 430 nm under Ar. Panel A shows the evaluation of the contribution from $(PS_4^{4-})^{\ddagger}$ to the observed decay curves in the aqueous and W20 solutions. Two solid curves show the calculated ones, $(TTA)_{calc}$, based on the simple TTA kinetics (eq 5′). The difference absorbance obtained by subtracting $(TTA)_{calc}$ from the observed values for the two solutions are shown in the figure as "obs. − $(TTA)_{calc}$". Panel B shows the decay curves corrected by eliminating the contribution from $(PS_4^{4-})^{\ddagger}$ fitted to the intra- and intermicellar TTA kinetics (solid curves). The values of $A'(0)$ and k_{inter} were obtained to be 0.157 ± 0.001 and $(5.0 \pm 0.6) \times 10^7$ M^{-1} s^{-1} for the W50 solution by fitting the decay curve with eq 5′ in the temporal range between 15−25 and 86 μs, where $\epsilon = 17\,000 \pm 1000$ and $L = 0.29 \pm 0.02$. The calculated curves with the combined decay function derived from the intra- and intermicellar TTA kinetics reproduced well the observed curves ($R^2 = 0.9598$ for the W50 solution).

Na_4PS_4. T−T absorption of Na_4PS_4 showed a definite peak at 430 nm in aqueous solution. This peak, however, involved a significant contribution from a minor transient species in addition to the T−T absorption as shown in Figure 1A. The transient, with a lifetime of about 1.5 μs and an intensity of about 5% of the total absorbance, was probably attributable to the unrelaxed state, $(PS_4^{4-})^{\ddagger}$, formed immediately after the fluorescence was emitted. The existence of such an intermediate was experimentally confirmed in the case of NaPS.[8] Figure 1A also shows that $(PS_4^{4-})^{\ddagger}$ participated in the decay curve observed in AOT reverse micellar solution with $W = 20$ (abbreviated as W20 solution). The contribution from this transient was very similar in both aqueous and W20 solutions. Thus, the contribution from $(PS_4^{4-})^{\ddagger}$ can rationally be eliminated with the same

exponential decay function. Furthermore, it was found that the absorbance at $t = 0$, that is, the yield of triplets, was not changed in the micellar solution. The corrected decay curves after eliminating the contribution from $(PS_4^{4-})^{\ddagger}$ were thoroughly described by the bimolecular triplet−triplet annihilation (TTA) kinetics. Figure 1B demonstrates the W dependence of the decay curves in the range from $W = 30$ to $W = 50$. It was found that the T−T absorption observed in solutions containing such a large reverse micelle did not decay according to the simple bimolecular TTA mechanism but apparently involved two types of triplet species with different decay rates. The fast one was found to strongly depend on W. This component is attributable to the intramicellar TTA as previously reported in different micellar systems.[10] The slower one was considered to be not due to the natural decay but the intermicellar TTA because the decay rates of this component also depended on W, [probe], and temperature.[20] Thus, we analyzed the observed decay curves with the following two TTA kinetics: (i) intermicellar TTA ($m_i \neq m_j$; rate constant = k_{inter})

$$(T)_{m_i} + (T)_{m_j} \rightarrow (T)_{m_i \text{ or } m_j} + (S0)_{m_j \text{ or } m_i} \quad (1a)$$

$$(T)_{m_i} + (T)_{m_j} \rightarrow (S0)_{m_i} (\text{or } (S1)_{m_i}) + (S0)_{m_j} \quad (1b)$$

(ii) intramicellar TTA (rate constant = k_{intra})

$$(T)_{m_i} + (T)_{m_i} \rightarrow (T)_{m_i} + (S0)_{m_i} \quad (2a)$$

$$(T)_{m_i} + (T)_{m_i} \rightarrow (S0)_{m_i} (\text{or } (S1)_{m_i}) + (S0)_{m_i} \quad (2b)$$

where S1 and subscripts of m_i and m_j indicate the excited singlet species and ith and jth micelles, respectively.

The intramicellar TTA could naturally be neglected if the probe molecules were completely dispersed, that is, in micelles in which the average number of probe molecules per micelle ($\langle n \rangle$) is much less than 1. In fact, no significant contribution from the intramicellar TTA was detected in $W20$ solution. The value of $\langle n \rangle$ in this micellar solution was estimated to be ca. 0.3 using the relation $\langle n \rangle = [\text{probe}]/([\text{AOT}]/N_{ag})$ where N_{ag} was the average aggregation number of surfactants per micelle reported previously.[21] In a micelle containing more than two probe molecules, the intramicellar TTA could occur and then finally only one or zero triplet remained in the micelle depending on the type of reaction (eq 2a or 2b) and the initial distribution of triplets. The concentration of the surviving triplet relative to the initial one, T(∞)/T(0), can easily be derived when we assume a Poisson distribution for probe molecule.[10] Two different relations 3a and 3b were obtained for the TTA processes of eqs 2a and 2b, respectively:

$$T(\infty)/T(0) = (1 - e^{-\langle n \rangle \alpha})/(\langle n \rangle \alpha) \quad (3a)$$

$$= (1 - e^{-2\langle n \rangle \alpha})/(2\langle n \rangle \alpha) \quad (3b)$$

where α is the yield of triplets and thus $\langle n \rangle \alpha$ (T_{av}) is the average number of triplets per micelle. From the relations 3a and 3b,

$$\{T(\infty)/T(0)\}_{2a}/\{T(\infty)/T(0)\}_{2b} \cong 2 \quad (4)$$

when $\langle n \rangle \alpha > 1$.

Because the intramicellar TTA process in a micelle containing more than two triplets proceeds more rapidly than the intermicellar one, the triplets could initially be quenched through the intramicellar process and subsequently the surviving triplets decay according to the intermicellar one, that is, reactions 1a or 1b. The decay function for this intermicellar TTA is given by eq 5.

$$T_s(t) = T'(0)/\{1 + k_{inter} T'(0) t\} \quad (5)$$

Because $A(t) = \epsilon T_s(t) L$ ($A(t)$ = absorbance at t, ϵ = molar extinction coefficient, L = effective optical path length), eq 5 can be transformed into eq 5′.

$$A(t) = A'(0)/\{1 + k_{inter} A'(0) t/(\epsilon L)\} \quad (5')$$

The observed decay curves were analyzed by the following fitting procedures: (1) First, we derived the decay curves $T_c(t)$ attributable purely to the T−T absorption by subtracting the contribution due to $(PS_4^{4-})^{\ddagger}$, which was evaluated with the same exponential decay function independent of W as mentioned above. (2) Second, we fitted the corrected decay curves $T_c(t)$ to eq 5′ in the temporal range where the contribution from the intramicellar TTA processes could be neglected, for example, $t \geq 20$ μs for $W50$ solution in Figure 1B. In this procedure, we can obtain the rate constant k_{inter}, as well as the approximate concentration of the surviving triplet T(∞) by assuming T(∞) ≅ T′(0) in eq 5. (3) Finally, the decay curves of the residual triplets, $T_c(t) - T_s(t)$, were analyzed on the basis of the intramicellar TTA kinetics. The decay function was given by eq A6 in the Appendix. The value of T(0) involved in this equation, that is, the initial concentration of triplets, was assumed to be equal to the initial concentration of triplets in aqueous solution as mentioned above. In this procedure, we can obtain the rate constant k_{intra}, as well as the average number of triplets per micelle, $\langle n \rangle \alpha$.

The yield of triplets (α) was independently determined from the absorbance at 430 nm observed as a function of [PTS], [AOT], W, and L using $\epsilon = 17\,000 \pm 1000$.[8] The obtained value of α was relatively large (0.42 ± 0.02), suggesting the efficient formation of triplets in PS_4^{4-}. By using two values of $\langle n \rangle \alpha$ and α determined with independent methods, we are able to estimate the average number of probe molecules per micelle, $\langle n \rangle_{T-T}$, that differ in the quenching mechanisms 2a and 2b. These values of $\langle n \rangle_{T-T}$ were compared with $\langle n \rangle$ estimated from the average aggregation number of surfactants per micelle (N_{ag}).[21] The results are shown in Figure 2. It is clear that the values of $\langle n \rangle_{T-T}$ obtained by assuming the reaction 1a (or 2a) are approximately equal to $\langle n \rangle$. Therefore, the dominant TTA mechanism of the PS_4^{4-} triplet can be represented by reaction 1a (or 2a): T + T → T + S0. This TTA mechanism is consistent with the findings that no delayed fluorescence was detected for the Na_4PS_4 probe molecule in contrast with the case of NaPS.[22]

NaPS. The T−T absorption peak was observed at 420 nm in both aqueous and micellar solutions. This peak for NaPS was mainly attributable to T−T absorption but was contaminated by several transients such as cation radicals, anion radicals, some unknown photoproducts (or their intermediates), and $(PS^-)^{\ddagger}$ when the measurements were done under an inert atmosphere (Ar) with a high-power laser. To eliminate the transients formed via the two-photon process, that is, $P^{\bullet+}S^-$, $P^{\bullet-}S^-$, and photoproducts, we measured the transient absorption at as low a laser power as possible. Under this condition, the observed decay curves contained only two transients at any wavelength: $(PS^-)^{\ddagger}$ and triplets. The former decays are described by an exponential decay function, while the latter ones obey the TTA process given by T + T → T + S0 or T + T → S0 (or S1) + S0. The decay curves observed in the $W50$ solution were decomposed into the two transients with the fitting function of $\{A_1 \exp(-k_1 t) + A_2/(1 + A_2 k_2 t)\}$. The TA spectra of the two species after 1.2 μs

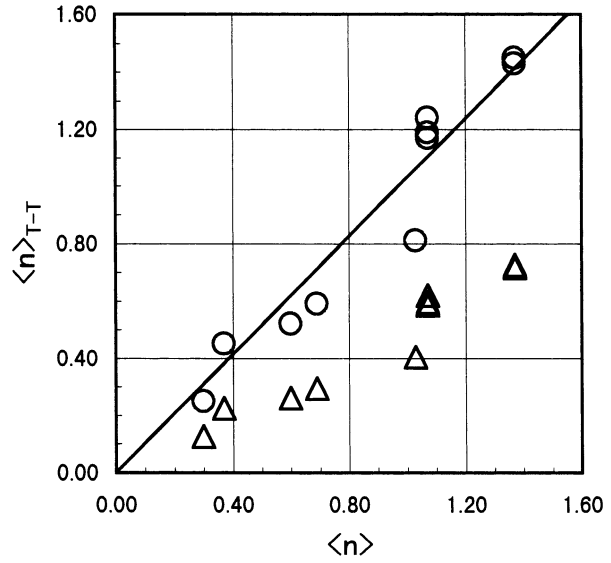

Figure 2. Correlation between $\langle n\rangle_{T-T}$ and $\langle n\rangle$. The values of $\langle n\rangle_{T-T}$ were calculated with two TTA models: T + T → T + S (○) and T + T → S + S (△). The solid line shows the least-squares fitting curve for the former model: $\langle n\rangle_{T-T} = (1.03 \pm 0.04)\langle n\rangle$.

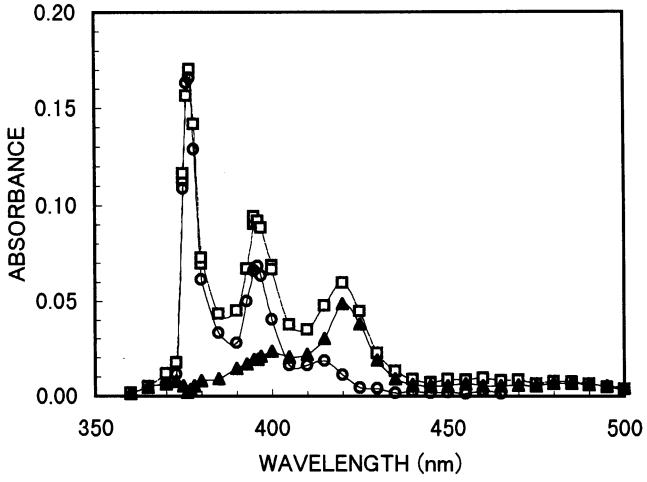

Figure 3. Deconvolution of TA spectra of NaPS in the *W*50 solution. The TA spectrum observed at 1.2 μs with a weak energy of laser (0.8 mJ) under Ar was shown as empty squares. The decay curves observed at each wavelength were decomposed into two components and the calculated absorbances at 1.2 μs were plotted: $(PS^-)^‡$ (○) and triplet (▲).

are shown in Figure 3. The spectrum attributable to $(PS^-)^‡$ is in agreement with that in aqueous solution reported previously.[8] From this spectrum, the relative intensity A_{420}/A_{375} was estimated to be 0.10. The lifetimes of $(PS^-)^‡$ were nearly constant (1.3−1.4 μs) in the spectral range from 375 to 430 nm. On the other hand, the absorbance at 375 nm due to T−T absorption was negligibly small. Thus, the contamination at 420 nm due to the $(PS^-)^‡$ transient can easily be eliminated. The corrected decay curves for T−T absorption can be fitted by only the slow TTA process, while the rapid intramicellar TTA process was not observed under this condition. This is due to the extremely small number of triplets per micelle, estimated to be about 0.03.

When the decay curves were measured with a sufficiently high laser power, adequate to produce more than two triplets per micelle, TA at 420 nm would involve two-photon transients as mentioned previously, in addition to T−T absorption and $(PS^-)^‡$. The radical anion $P^{\bullet-}S^-$, detectable at 490 nm in aqueous solution, was a very minor species even in the *W*50 solution. Therefore, the contribution of this transient could be neglected at 420 nm. The unknown species with a long lifetime were roughly estimated from the decay curves observed in solutions containing KI under O_2, in which both cation radicals and triplets of PS^- were quickly quenched in a few hundred nanoseconds. If the TA spectra of cation radicals were assumed to be the same as that in aqueous solution reported in ref 8, the intensity at 420 nm relative to that at 460 nm, $(I_{420}/I_{460})_{cation}$, was estimated to be 0.22. An example for the decay curve of pure T−T absorption, corrected by subtracting three contaminants, $(PS^-)^‡$, $P^{\bullet+}S^-$, and photoproducts, is shown in Figure 4. This decay curve was never reproduced only by the intermicellar TTA. The residual intensity was attributable to the intramicellar TTA as confirmed in the case of PS_4^{4-}. The corrected decay curve was analyzed by fitting to the decay function involving both intra- and intermicellar TTA. The estimated value of $\langle n\rangle\alpha$ was 0.12 and 0.24 for the two TTA mechanisms (eqs 1a + 2a and 1b + 2b, respectively). By using $\alpha = 0.082$ (observed value) and $\epsilon = 23\,000 \pm 1000$,[8] we estimated the values of $\langle n\rangle_{T-T}$ to be 1.5 and 3.0, respectively. The latter value of $\langle n\rangle_{T-T}$ (3.0) is significantly larger than the value of $\langle n\rangle = 1.4$,[21] even if a considerable accumulated error was taken into account. Therefore, it appears very likely that triplets of PS^- are dominantly quenched according to the reaction 1b or 2b, that is, T + T → S1 + S0, S1 → S0 + $h\nu$. This mechanism can also explain the observed strong delayed fluorescence.[22]

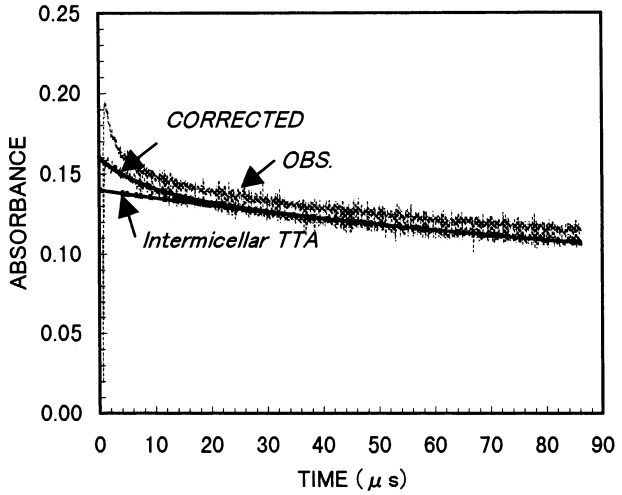

Figure 4. Decay curve of PS^- triplets in the *W*50 solution observed at 420 nm under Ar. The corrected decay curve ("corrected") was obtained by eliminating the contributions from three possible transient species other than the triplets (see the text). The two solid curves show the fitting curves with the combined kinetics of intra- and intermicellar TTA and only intermicellar TTA kinetics ($R^2 = 0.9939$ for the former fitting curve).

HPB. The observed decay curves of triplets of HPB in AOT micellar solution showed no significant dependence on *W* and were very similar to those observed in aqueous ethanol solution. The decay curves were described by a simple TTA kinetics, probably intermicellar TTA. Because HPB is insoluble in water, as well as isooctane, HPB could be located in a micelle. Therefore, it appears that HPB triplets located in a micelle show the quenching behavior similar to those in aqueous ethanol solution.

2. Cation Radical. Cation radicals formed from two pyrene derivatives (NaPS and HPB) in micellar solution gave an absorption maximum at 460 nm, while the cation radical from Na_4PS_4 showed a strong peak at 505 nm, in addition to a shoulder-like peak at 460 nm. In ref 8, we confirmed that the

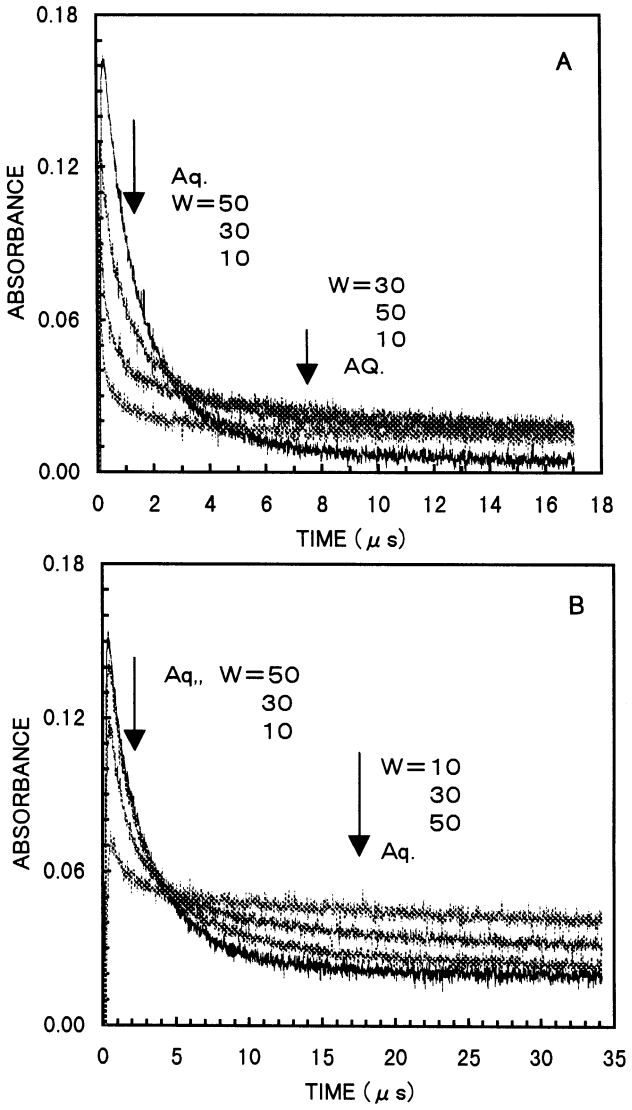

Figure 5. *W* dependence of decay curves of transient species from PS^- monitored at 460 nm under O_2 (A) and N_2O (B). The decay curve for the *W*40 solution under N_2O (data not shown) completely overlaps with the curves for the *W*50 and aqueous solutions in the temporal range shorter than 5 μs.

cation radicals from PS^- and PB^- were zwitterions and dominantly quenched by the following bimolecular process: $P^{\bullet+}S^- + PS^-$. This means that the micellar effects could be expected for the decay process of these cation radicals.

NaPS in AOT Reverse Micelle. Figure 5 shows the *W*-dependent decay curves at 460 nm observed under O_2 and N_2O atmospheres. These decay curves involve a significant contribution from T−T absorption, as shown in the TA spectra of triplet of PS^- (Figure 3). This contribution was estimated to be about 0.02 in absorbance units at $t = 0$ for all of the decay curves using the relative intensity of $(A_{460}/A_{420})_{triplet}$ (0.11−0.12 in Figure 3) and the corrected absorbance at 420 nm due purely to the triplet measured under the same condition (approximately 0.16−0.17, in Figure 4). This is consistent with the decay curve observed in aqueous solution under N_2O in Figure 5B, which remained almost constant (about 0.02) even after the cation radicals rapidly decayed. Under O_2, the triplets were thoroughly annihilated within 0.2−0.4 μs. The decay curves in the temporal range ($t \geq 0.5$ μs) at which contribution from triplets was negligibly small could be fitted by neither single-exponential decay kinetics nor second-order ones but by biexponential decay functions. It is likely that there exist two transients at least with different lifetimes. Both species were attributable to the cation radicals because those were rapidly quenched by I^- anions. The lifetimes of the fast-decaying species $(P^{\bullet+}S^-)_{short}$, as well as the overall yields of the cation radicals ($(P^{\bullet+}S^-)_{short} + (P^{\bullet+}S^-)_{long}$), were found to decrease with a decrease in *W*. This trend was closely related to that of hydrated electrons under Ar, monitored at 700 nm. The overall yield of $P^{\bullet+}S^-$ increased by 0.02−0.05 in absorbance units when the atmosphere was changed from O_2 to N_2O. The relative yield was also varied in association with this atmospheric change, which was strongly dependent on *W*. As shown in Figure 5B, the yields observed in *W*50 and *W*40 solutions increased to be comparable with that in aqueous solution. Those were mainly due to the increase in $(P^{\bullet+}S^-)_{short}$. On the other hand, the increase in *W*10 solution was predominantly due to the increase in $(P^{\bullet+}S^-)_{long}$. Such an enhancement effect by N_2O can essentially be explained by considering that N_2O molecules can effectively capture the solvated electrons produced in a reverse micelle and thereby prevent the recombination reaction between the solvated electrons and the cation radicals. The observed *W* and atmospheric dependence of the overall yield of $P^{\bullet+}S^-$ can be understood on the basis of the competitive capture, reactions of solvated electrons by the cation radicals and the other effective quenchers such as N_2O and water (pool). In a small water pool, the recombination reaction with the cation radical so rapidly occurs that the trapping effect with N_2O or the water pool is less efficient. Therefore, the overall yield is relatively small for small *W* solutions.

This model, however, did not explain the presence of two kinds of cation radicals, $(P^{\bullet+}S^-)_{short}$ and $(P^{\bullet+}S^-)_{long}$, and the *W* dependence of the relative yield. Here, we present the two distinct locations model of PS^-, in which the fast decay species exists in a water pool and the slow decay one is formed by ionization of PS^- located in the surfactant palisade layer. This may partly be supported by the solubilization test of NaPS. This molecule is considerably soluble in pure water but begins to precipitate in a highly ionic solution, for example, ≥ 2 M $NaClO_4$ solution. The water pool in a micelle with a small value of *W*, for example, $W = 10$, is very small and too highly ionic to solubilize NaPS. As a result, most PS^- molecules should be expelled from the water pool but stay in the palisade layer because its sulfate group is strongly anchored on the polar layer of the micelle. On the other hand, in a large water pool, PS^- molecules should be distributed mainly in the water pool and partly in the palisade layer. Furthermore, a small water pool is not an effective medium as an electron trap, so the charge separation hardly occurs, leading to a decrease in the yield of cation radicals.[11] The *W*-dependent two distinct locations model can also explain the experimental results that the fluorescence lifetime of NaPS decreased from 110 ns (109 ns reported previously[23]) to 92 ns with an increase in *W* from 4 to 50, which was longer than that obtained in aqueous solution (65 ns, 64 ns[23]). Additional evidence was presented in the preliminary results that the lifetime of $P^{\bullet+}S^-$ isolated in a hydrophobic region of a micelle consisting of SDS became markedly lengthened.[24]

Figure 6 shows the [NaPS] dependence of rate constants obtained for the fast-decaying $P^{\bullet+}S^-$ observed in *W*50 solution under O_2. The decay constants were found to be almost constant below $(6-8) \times 10^{-5}$ M ($[NaPS]_C$). This presents a striking contrast to the decay constants obtained in aqueous solution, which linearly depend on [NaPS]. The result indicates that the $P^{\bullet+}S^-$ cation radicals in the *W*50 solution below $[NaPS]_C$ decay obeying the unimolecular mechanism (not the bimolecular one). This change in the quenching mechanism is consistent with the

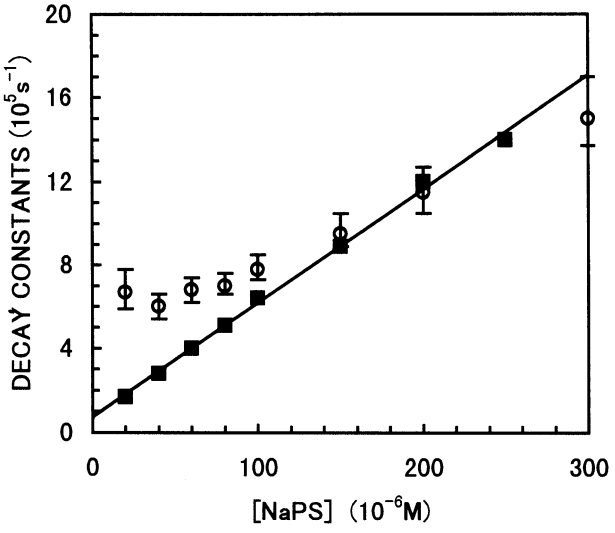

Figure 6. [NaPS] dependence of the decay constants of $P^{\bullet+}S^-$ cation radical in aqueous (■) and *W*50 (○) solutions under O_2. The decay constants in micellar solutions were plotted for the fast decay components, obtained by analyzing the decay curves at 460 nm with biexponential decay functions. The error bars were drawn by evaluating both the errors of the estimates in 95% confidence limits and the errors due to the ambiguities in the subtraction of T−T absorption from the observed decay curves. The decay constants in aqueous solutions were presented in the preceding paper as the following linear functions of [NaPS]: $(5.5 \pm 0.1) \times 10^9$[NaPS] + $(7 \pm 2) \times 10^4$. [8]

fact that $[NaPS]_C$ corresponds to the critical concentration below which $\langle n \rangle$ is reduced to less than unity. In micellar solutions with such a small $\langle n \rangle$, each PS^- molecule is considered to behave as an isolated molecule in a micelle when the intermicellar interaction can be neglected. Therefore, the micellar environment is likely the most dominant factor to determine the average decay constant below $[NaPS]_C$ ($(6.5 \pm 0.5) \times 10^5$ s^{-1}), which was about 1 order of magnitude larger than the decay constant extrapolated to the infinite dilution in the aqueous solution ($(7 \pm 2) \times 10^4$ s^{-1}).[8] This enhancement could reasonably be interpreted by an apparent increase in the ionic strength in a water pool. With a further increase in [NaPS], a micelle contains more than two PS^- molecules and the decay rate increases obeying the bimolecular quenching mechanism via intra- and intermicellar processes.

Na_4PS_4 in AOT Reverse Micelle. The cation radical produced from two-photon ionization of PS_4^{4-} exhibited an absorption maximum at 505 nm in aqueous solution. This transient decayed significantly more slowly than the cation radical of $P^{\bullet+}S^-$. The lifetime was very long (≤1 ms) under Ar, while it decreased by a factor of 15−20 under O_2. In a highly ionic solution composed of several typical salts such as $NaClO_4$, its decay rate was about 1 order of magnitude faster than in pure water.

Figure 7 shows the decay behavior of this species monitored at 505 nm as a function of *W*, as well as the atmosphere (Ar, N_2O, or O_2). In Figure 7A, the decay curves observed under Ar were found to strongly depend on *W* and converge toward the decay curve observed in *W*10 solution. This curve (W = 10) rapidly decayed under O_2 but was little affected in the presence of N_2O as shown in Figure 7B and also in the presence of KI (data not shown). This means that the detected signal in the *W*10 solution is wholly attributable to the T−T absorption without any contribution from the cation radicals. In fact, the TA spectra in the *W*10 solution under Ar, as shown in Figure 8, were in agreement with the TA spectra of triplet of PS_4^{4-} in aqueous solution (Figure 2B in ref 8). In micellar solutions with $W \geq 20$, a rapidly decaying component appeared and the yields

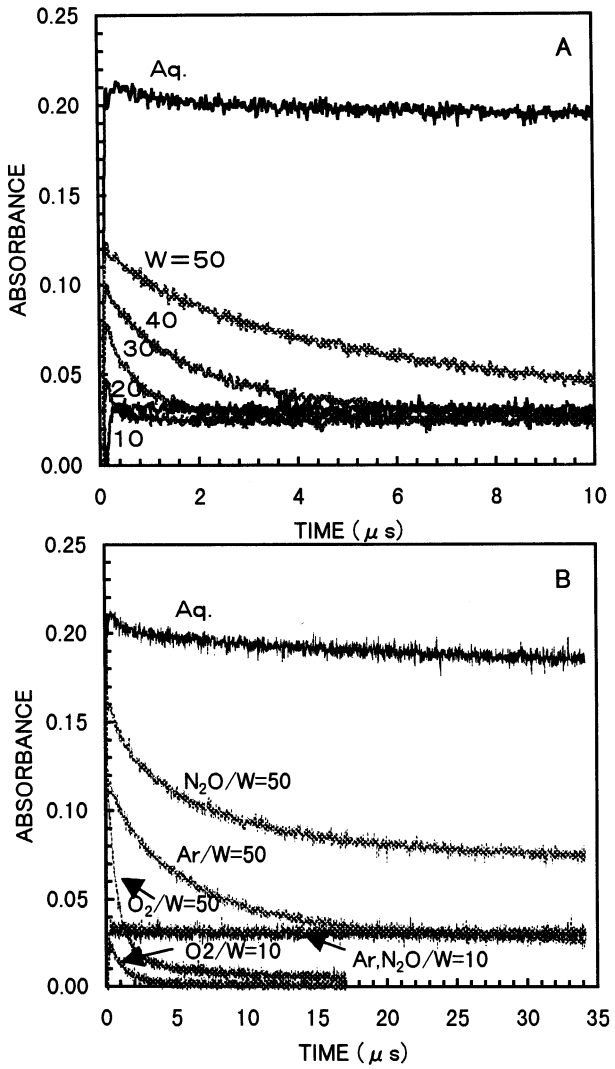

Figure 7. *W* and atmosphere dependence of decay curves of transient species from PS_4^{4-} observed at 505 nm: (A) *W* dependence under Ar; (B) atmosphere (Ar, N_2O and O_2) dependence in *W*50 and *W*10 solutions.

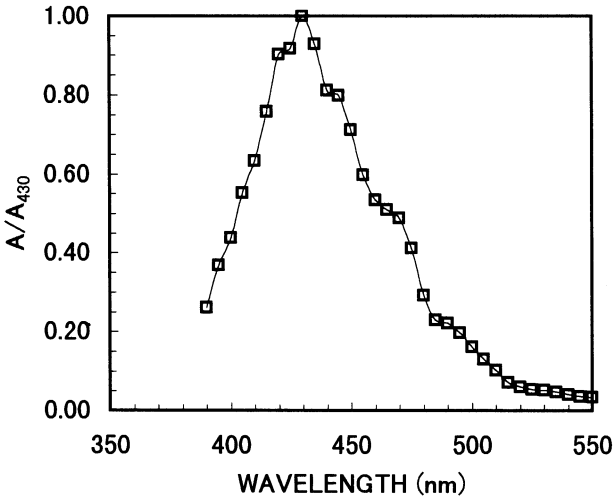

Figure 8. Normalized TA spectra of PS_4^{4-} in the *W*10 solution under Ar. The absorbance values normalized to that at 430 nm (A/A_{430}) were the averaged values obtained in the temporal range from 5 to 50 μs.

increased with the increase in *W*. Figure 7B clearly shows that the lifetime in the *W*50 solution observed under O_2 markedly decreased in comparison with that under Ar. This trend is

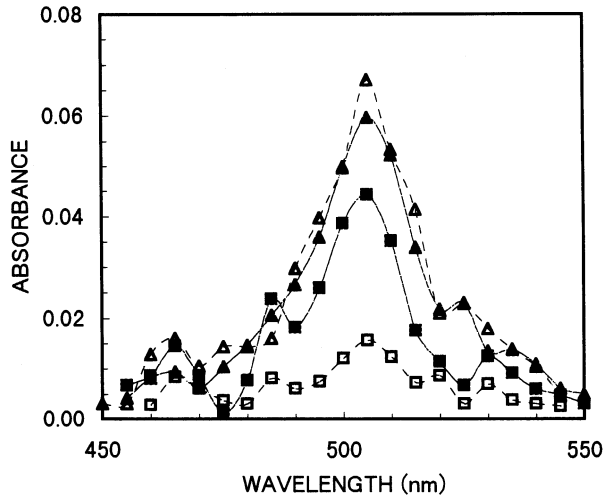

Figure 9. TA spectra of two kinds of cation radicals having short and long lifetimes produced from PS_4^{4-}. Filled and empty triangles represent the absorbance values at 1 μs under N_2O and Ar, respectively, which are attributable to the cation radicals with a short lifetime. Filled and empty squares represent those with a long lifetime under N_2O and Ar at 50 μs, respectively. The observed decay curves, corrected by eliminating the contribution from T−T absorption, were fitted with biexponential decay functions.

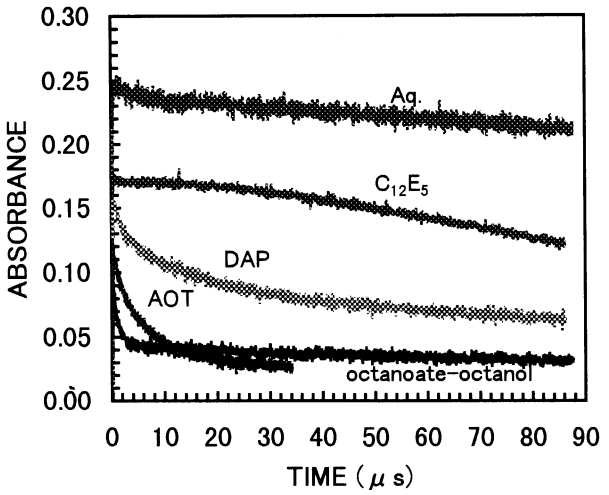

Figure 10. Comparison of decay curves of transient species from PS_4^{4-} observed at 505 nm under Ar in four different micellar solutions (AOT, sodium octanoate−octanol, DAP, and $C_{12}E_5$).

essentially similar to that in aqueous solution. The decay behaviors observed under N_2O are very interesting. Figure 7B shows that the absorbance in the *W*50 solution increased in a parallel displacement when the atmospheric gas was changed from Ar to N_2O. The constant increments were also attributed to the cation radical species because those were quenched by I^- anions. Such N_2O effects are quite different from those on $P^{\bullet+}S^-$ cation radicals, for which the increase was dominantly due to the rapidly decaying component in the *W*50 solution. The decay curve entirely attributable to the cation radicals was deduced by subtracting the contribution from the T−T absorption, which was estimated from the relative intensity of A_{505}/A_{430} (0.13) in Figure 8 and the corrected decay curve at 430 nm (see Figure 1). Those were well fitted using a biexponential decay function with two different lifetimes. The spectra of the two components, as shown in Figure 9, were very similar in the wavelength range from 450 to 550 nm. Therefore, the two species are considered to resemble each other in their electronic structures. However, the chemical properties appear to be quite different because their quenching behaviors by N_2O were opposite: the slowly decaying species can be revived by N_2O, while another species with a short lifetime was little affected by N_2O. Because N_2O is an effective quencher of hydrated electrons, the slowly decaying ones are considered to be the species that are easily quenched by hydrated electrons. In the presence of N_2O, the hydrated electron is immediately captured by N_2O and then the cation radical remains alive.

To obtain further information on the cation radicals from PS_4^{4-}, we measured the decay curves in three reverse micellar systems different from AOT. The results are summarized in Figure 10. The first reverse micelle, prepared from sodium octanoate ($C_7H_{15}COONa$) as an anionic surfactant and *n*-octanol ($C_8H_{17}OH$) as both a cosurfactant and a cosolvent, is expected to form a water pool similar to that of AOT reverse micelle. In this micelle, the initial decay was observed to be steeper than that of the AOT reverse micelle ($W = 50$). This is consistent with the finding that the size of the water pool, estimated to be ca. 4 nm in radius,[25] was as small as that of the AOT reverse micelle between $W = 20$ and 30. Strictly speaking, the decay constant is comparable with that of $W = 40$. This discrepancy may be explained by the dilution effect due to the cosurfactant, as well as the small dissociation constant of the surfactant, leading to decreases in ionic strength in this water pool. The second case was a reverse micelle composed of DAP. The water pool of this reverse micelle is known to be very small (ca. 2 nm in radius),[19,26] which is comparable with that of AOT with $W = 10$. Nevertheless, a considerably large absorbance at $t = 0$ and a significant contribution of the slowly decaying component was observed, while no signals attributable to the cation radical were detected in the AOT reverse micelle with $W = 10$. A simplified representation of this micelle shows that the water pool is enveloped by the surfactant layer where dodecylammonium cation and propionate anion are arranged with each other and strongly coupled. As a result, the interface is polar but the ionic strength inside the water pool is very low. The latter property is quite different from the former two water pools. These properties of the water pool may affect the formation and the decay behavior of the cation radicals. Finally, we compared the decay curve observed in a reverse micelle from nonionic surfactant of $C_{12}E_5$. The water pool of this reverse micelle is rather small, maybe 4−5 nm,[27] and is enclosed with a neutral interface. The observed decay curve showed that the rapidly decaying component disappeared in the temporal range investigated (>50 ns). Furthermore, it was found that the decay curve could not be described by simple exponential decay kinetics. In addition, the decay curves observed in the latter two micelles were not affected in the presence of N_2O. These results suggest that the kinetics on formation and decay of the cation radicals from Na_4PS_4 are dominated by not only the size of the water pool but also the physicochemical nature of the water pool such as ionic strength and interface polarity.

The rapid decay behavior of the cation radical was also detected in aqueous solutions containing several specific anions: I^-, SO_3^{2-}, and OH^-.[8] However, the former two anions were not involved in the water pool of the reverse micelles investigated. The significant effect of OH^- was also neglected because the pH of the water pool was confirmed to be slightly acidic by the pH indicator of pyranine. Hasegawa recently provided several evidences that pH of the water pool in the AOT reverse micelle is maintained at about 5 through the buffer action of AOT molecules.[6] This means that $[OH^-]$ is too low to induce such a rapid decay in the water pool. Therefore, the cation radical produced in the water pool may obey a different

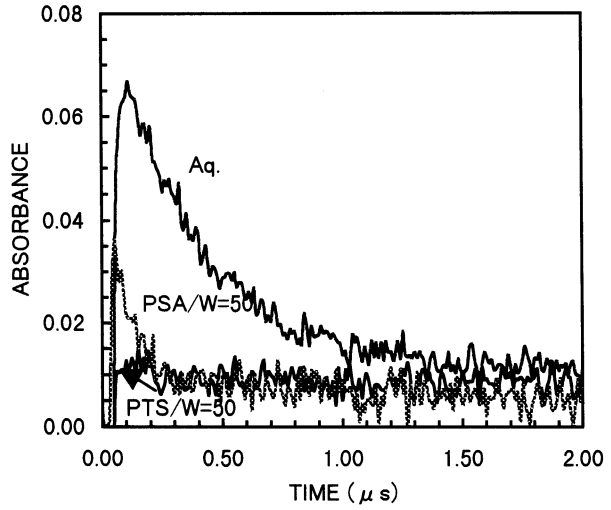

Figure 11. Decay curves of solvated (hydrated) electrons monitored at 700 nm. The solvated electrons were generated by laser irradiation of NaPS in *W*50 solution or Na_4PS_4 in aqueous and *W*50 solutions.

quenching mechanism or may be a quite different species from the common cation radical $P^{\bullet+}S_4^{-4-}$ compared with $P^{\bullet+}S^-$.

First, we considered that the surfactant molecules acted as effective nucleophilic quenchers. Grand[14] adopted this quenching mechanism to interpret the *W*-dependent decay behaviors of the cation radical of tetramethylbenzidine in the AOT reverse micelle. The decay of this cation radical, however, proceeds significantly more slowly (in millisecond time scale) than that of the cation radical from PS_4^{4-} (in microseconds). Furthermore, the $CH_3SO_3^-$ anion, an analogous molecule of AOT, was known to be a poor quencher of the cation radical.[8] Thus, this mechanism is improper for the present case.

Second, the distinct location model is considered. This model can successfully explain the decay behaviors of $P^{\bullet+}S^-$ as mentioned above. This model, however, is also improbable because PS_4^{4-} anions are distributed within the water pool. It is unlikely that the cation radicals formed by ionization of PS_4^{4-} molecules located at the two distinct sites of the water pool with different ionic environment, that is, the central site and peripheral one, could decay through different quenching processes.

Finally, we considered the case that the cation radicals showing rapid and slow decays are different species in their chemical properties. It is reasonably assumed that the slowly decaying species is the common cation radical, that is, $P^{\bullet+}S_4^{4-}$, which is formed via complete charge separation. This species could easily be quenched by hydrated electrons existing in the same water pool. Therefore, an effective quencher for hydrated electrons such as N_2O or bulk water or both is required to ensure the detection of this species. Formation of the rapidly decaying species is characteristic of the water pool with an appropriate ionic environment. One possible model for this species is proposed: an intramolecular charge-separated molecule presented as $(S^-)_3P^{\bullet+} \rightarrow S^{2-}$. This species also has the $P^{\bullet+}$ cation radical center similar to $P^{\bullet+}S_4^{4-}$, resulting in similar absorption spectra. This proposal may partly be supported by the following findings: (1) The hydrated electron was undetectable within the temporal range investigated after laser irradiation ($\geq$50 ns) when the AOT reverse micellar solution containing PS_4^{4-} was irradiated. This result presents a striking contrast to the case of PS^- containing solution in which a considerable amount of hydrated electrons were detected, as shown in Figure 11. (2) The lifetime of this cation radical was markedly reduced in the presence of O_2 as shown in Figure 7B. This suggests that the cation radical is not a simple doublet one such as $P^{\bullet+}S^-$. (3) This cation radical can be detected only in an appropriate ionic environment, which is consistent with the general trend that the charge-transfer state is stabilized in a highly dielectric medium.

This species would decay via several routes: electron emission (formation of $P^{\bullet+}S_4^{4-}$ and solvated electron), intramolecular charge recombination (regeneration of PS_4^{4-}), and decomposition into some photoproducts such as pyranine. Kinetic analysis was tried according to the scheme involving the formation of two kinds of cation radicals and the decay routes mentioned above. The results, however, were very qualitative because many unknown parameters were involved. Nevertheless, it appears that the feature of the decay curves observed under various conditions can be interpreted within this kinetic model.

3. Anion Radicals and Hydrated Electrons. To produce anion radicals in a water pool, more than two probe molecules should be distributed in a water pool, taking account of the lifetime of hydrated electrons. Therefore, it is considerably rare that the anion radical is formed in a water pool. A small but significant amount of the anion radical has been detected only in AOT reverse micelles containing NaPS,[16] while a considerable amount of hydrated electrons with short lifetimes were detected in a micelle containing NaPS and HPB. This result is consistent with the two distinct locations model of PS^-. When an electron is emitted into the water pool thorough ionization of the PS^- molecule in the palisade layer another PS^- molecule in the water pool will very likely capture this hydrated electron, leading to the formation of the anion radical.

Discussion

In these studies, our efforts have mainly been addressed to derive the pure spectrum of the transient target species from observed TA spectra, which are generally contaminated by multiple transient species, and to elucidate their decay mechanism, which sensitively reflects the microenvironment around those transient species. In this sense, our primary objects have successfully been achieved although both the probing and micellar systems investigated are limited. The methodology for its extension was established throughout these studies. Here, we briefly summarize the results and discuss what information is generally gained on the properties or dynamics or both of micellar systems when those transient species are employed as a probe. The following two probes are exemplified: (1) TTA process and (2) formation and quenching of cation radicals.

TTA Process. The pure T−T absorption spectra of Na_4PS_4 and NaPS in aqueous and micellar solutions can be separated from the observed TA spectra using the well-defined method to subtract the contribution of the other transient species such as cation radicals. Particularly in the case of Na_4PS_4, the correction was very simple and reliable because the contribution of other transient species to the T−T absorption maximum at 430 nm was very small. In addition, a reliable molar extinction coefficient of T−T absorption at 430 nm was obtained. Furthermore, the TTA mechanism of this probe was found to be represented by the reaction $T + T \rightarrow T + S0$. Therefore, the TTA processes of Na_4PS_4 have now been analyzable at a highly accurate level. The TTA processes of this probe in the water pool of the reverse micelle can be divided into two regimes of intramicellar and intermicellar TTA when no additional effective quenchers such as O_2 molecules coexist. From the analysis based on the former process, we can estimate the average number of probe molecules per micelle, that is, the average aggregation

number of surfactants per micelle. However, this analysis is meaningful only when more than two triplets are simultaneously produced in a micelle after laser irradiation. Therefore, a reverse micelle containing a considerably large water pool, for example, $W > 20$ micelle for the AOT reverse micellar system, should be required. On the other hand, the intermicellar TTA process is apparently independent of the size of the water pool but is related to the number of micelles containing more than one triplet relative to the total number of micelles. This process is considered to occur via the fusion−fission process between micelles, which is sensitive to the softness of the micellar shell. Therefore, the intermicellar TTA process is strongly affected by temperature and some cosurfactants added.[28−30] In a future publication, we will report the temperature and cosurfactant dependence of the intermicellar TTA process in this respect. The availability of this probe may be comparable with the fluorescence quenching method.

HPB is a rather hydrophobic probe with a polar substituent (−COOH). And then, this probe is easily solubilized into a reverse micelle. The TTA process of HPB solubilized in an AOT reverse micelle proceeds very slowly, and its kinetics can be described by intermicellar TTA. The rate constants were little dependent on *W*, suggesting that the intramicellar TTA, which may occur via triplet migration within the palisade layer, is negligible. NaPS is of an intermediate nature between Na_4PS_4 and HPB. In a reverse micelle containing a large water pool, PS^- probes appeared to be distributed in both the water pool and palisade layer. Nevertheless, the TTA process appears to resemble that of Na_4PS_4. This can be interpreted on the basis of the relatively rapid exchange of PS^- between the water pool and the palisade layer in addition to the slow diffusion within the palisade layer.

Formation and Quenching of Cation Radicals. The TTA process is sensitive to the distribution of the probe molecule, leading to determination of the aggregation number of micelles. On the other hand, cation radicals may be very useful probes reflecting the nature of the microenvironment in addition to the size parameter. This can be realized in the observed decay profiles that complicatedly depend on both *W* and the nature of surfactant used. A marked *W* dependence of formation yield, as well as decay constant, of the cation radical was found. These results can be explained on the basis of the interrelated effects from the following three changes associated with a decrease in *W*: the decrease in charge-separation probability, the increase in charge-recombination probability, and the increase in ionic strength in the water pool. The former two probabilities are strongly dependent on the size of the water pool. In particular, the cation radical from Na_4PS_4 is more markedly affected because a photoejected electron and its product (cation radical) are forced to coexist within the same water pool. Experimental results have revealed that not only a completely charge-separated cation radical but an intramolecular charge-separated cation radical is formed in the two-photon ionization of Na_4PS_4 in the water pool. The latter cation radical is detected only in an ionic water pool, while a complete charge separation occurs in an aqueous or dilute ionic solution to produce the common $P^{\bullet+}S^{4-}$ species. The decay constant of the intramolecular charge-separated cation radical, however, was found to increase with the decrease in the water pool size, that is, the possible increase in the ionic strength in the water pool. This dependence leads to an empirical linear relation between the logarithm of the decay constant and the water pool size as shown in Figure 12. This relation has been examined only in AOT micellar systems. Grand derived a similar relation between *W* and the logarithm

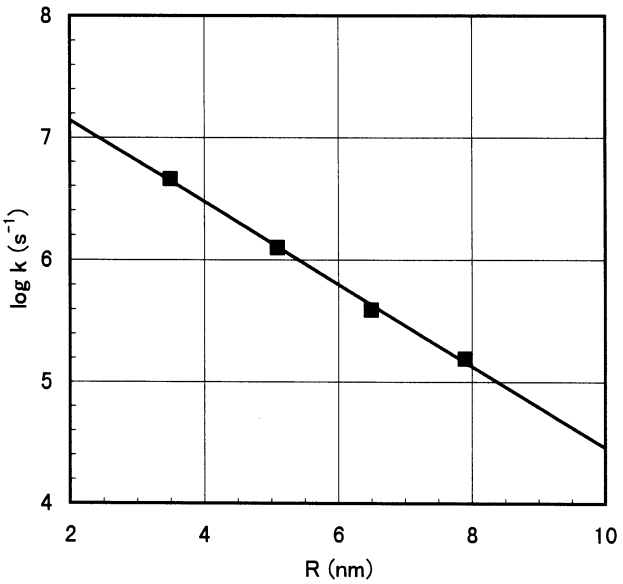

Figure 12. Relation between the radius of the water pool (*R*) and the decay constants of cation radicals with a short lifetime from PS_4^{4-}. The four values were obtained by analyzing the decay curves in *W*20, *W*30, *W*40, and *W*50 solutions observed under Ar. The sizes of WP are from previously reported values.[21a] The empirical relation shown as solid line was presented by the following equation: $\log\{k\ (s^{-1})\} = -(0.336 \pm 0.012)R + (7.812 \pm 0.069)$.

of decay constant of the tetramethylbenzidine cation radical in several reverse micelles involving AOT.[14] The observed decay profiles of the cation radical from Na_4PS_4 were found to exhibit a complicated dependence on the nature of surfactant used as shown in Figure 10. On the basis of the limited data obtained, it is suggested that the ionic properties surrounding the water pool may determine the relative contribution of the two cation radical species. When the surface is neutral, for example, reverse micelle from $C_{12}E_5$, the intramolecular charge-separated species are not produced or consecutively produce the completely charge-separated cation radical within a very short period. These results suggest that the decay behaviors of the cation radical from Na_4PS_4 provide useful information on the micellar microenvironment.

Acknowledgment. We thank M. Kobayashi for his assistance in preliminary measurements of TA spectra and analysis of the decay kinetics.

Appendix

The kinetic equations for intramicellar TTA processes 2a and 2b have been derived on the basis of the stochastic model. The pairwise annihilation reaction of triplets (eq 2b) was thoroughly solved by Rothenberger et al.[10] On the basis of their approach, we derived the kinetic equation for another TTA process, given by eq 2a. In reaction 2a, the differential-difference equations to be solved are given by A1.

$$dP_x(t)/dt = {}^1/_2 k_{intra}(x+1)xP_{x+1}(t) - {}^1/_2 k_{intra}x(x-1)P_x(t) \quad (x = 0, 1, 2, ...) \quad \text{(A1)}$$

where $P_x(t)$ is the probability that a micelle contains x triplets at time t and k_{intra} is the rate constant. By using the probability generating function $F(s,t)$, we can transform eq A1 into the following partial differential equation:

$$\partial F(s,t)/\partial t = {}^1/_2 k_{intra}(s - s^2)\,\partial F/\partial s \quad \text{(A2)}$$

A general solution of eq A2 is given by

$$F(s,t) = \sum_{n=0}^{\infty} A_n C_n^{-1/2}(2s-1)\exp\{-{}^1/_2 k_{\text{intra}} n(n-1)t\} \quad \text{(A3)}$$

where $C_n^{-1/2}(2s-1)$ is a Gegenbauer polynomial of degree n.

Here, the coefficient A_n can easily be calculated by assuming that $P_x(0)$ is given by a Poisson distribution as follows:

$$A_n = \frac{(1-2n)}{2^n} e^{-T_{\text{av}}/2} \sum_{m=0}^{\infty} \frac{\left(\frac{T_{\text{av}}}{2}\right)^{n+2m} \Gamma(m+{}^1/_2)}{(2m)!\Gamma(n+m+{}^1/_2)} \quad \text{(A4)}$$

where T_{av} and Γ are the initial number of average triplet per micelle and the gamma function, respectively. Because the average number of triplets per micelle at time t can be written as

$$\langle x(t)\rangle = [\partial F(s,t)/\partial s]_{s=1} = \sum_{x=1}^{\infty} x P_x(t) \quad \text{(A5)}$$

the concentration of triplets at time t relative to the initial one, $T(t)/T(0)$, is given by

$$T(t)/T(0) = \langle x(t)\rangle/T_{\text{av}} = -2/T_{\text{av}} \sum_{n=1}^{\infty} A_n \exp\{-{}^1/_2 k_{intra} n(n-1)t\} \quad \text{(A6)}$$

References and Notes

(1) Hansson, P.; Jönsson, B.; Ström, C.; Söderman, O. *J. Phys. Chem. B* **2000**, *104*, 3496.

(2) Kim, J.-H.; Domach, M. M.; Tilton, R. H. *Langmuir* **2000**, *16*, 10037.

(3) Prado, E. A.; Yamaki, S. B.; Atvars, T. D. Z.; Zimerman, O. E.; Weiss, R. G. *J. Phys. Chem. B* **2000**, *104*, 5905.

(4) Lissi, E. A.; Abuin, E. B.; Rubio, M. A.; Ceron, A. *Langmuir* **2000**, *16*, 178.

(5) Ruiz, C. C.; Aguiar, J. *Langmuir* **2000**, *16*, 7946.

(6) Hasegawa, M. *Langmuir* **2001**, *17*, 1426.

(7) Bales, B. L.; Ranganathan, R.; Griffiths, P. C. *J. Phys. Chem. B* **2001**, *105*, 7465.

(8) Mori, Y.; Shinoda, H.; Nakano, T.; Kitagawa, T. *J. Phys. Chem. A*, **2002**, *106*, 11743.

(9) Grätzel, M.; Kalyanasundaram, K.; Thomas, J. K. *J. Am. Chem. Soc*. **1974**, *96*, 7869.

(10) Rothenberger, G.; Infelta, P. P.; Grätzel, M. *J. Phys. Chem*. **1981**, *85*, 1850.

(11) Gauduel, Y.; Pommeret, S.; Yamada, N.; Migus, A.; Antonetti, A. *J. Am. Chem. Soc*. **1989**, *111*, 4974.

(12) Ghosh, H. N.; Sapre, A. V.; Palit, D. K.; Mittal, J. P. *J. Phys. Chem. B* **1997**, *101*, 2315.

(13) Grand, D.; Dokutchaev, A. *J. Phys. Chem. B* **1997**, *101*, 3181.

(14) Grand, D. *J. Phys. Chem. B* **1998**, *102*, 4322.

(15) Mori, Y.; Shinoda, H.; Kitagawa, T. *Chem. Phys. Lett*. **1991**, *183*, 584.

(16) Mori, Y.; Shinoda, H.; Kitagawa, T. *Chem. Lett*. **1993**, (1), 49.

(17) Politi, M. J.; Brandt, O.; Fendler, J. H. *J. Phys. Chem*. **1985**, *89*, 2345.

(18) Kitahara, K. *Bull. Chem. Soc. Jpn*. **1955**, *28*, 234.

(19) Correll, G. D.; Cheser, R. N., III; Nome, F.; Fendler, J. H. *J. Am. Chem. Soc*. **1978**, *100*, 1254.

(20) Mori, Y.; Kobayashi, M.; Shinoda, H.; Nakano, T. To be submitted for publication. A brief summary was reported by Mori, Y. et al. at p 276 in *Abstracts of International Conference on Colloid and Surface Science* (Tokyo, 2000).

(21) (a) Maitra, A. *J. Phys. Chem*. **1984**, *88*, 5122. (b) Eicke, H.-F.; Rehak, J. *Helv. Chim. Acta* **1976**, *59*, 2833. In this work, we employed the following N_{ag} values based on the tabulated data in ref 21a: $N_{\text{ag}} = 98$, 302, 613, 965, and 1380 for *W*10, *W*20, *W*30, *W*40, and *W*50 solutions, respectively. Thus, $\langle n\rangle = 0.10$, 0.30, 0.61, 0.97, and 1.4 for *W*10, *W*20, *W*30, *W*40, and *W*50 solutions when [probe] $= 1.0 \times 10^{-4}$ M and [AOT] $= 0.10$ M.

(22) Bohme, C.; Abuin, E. B.; Scaiano, J. C. *J. Am. Chem. Soc*. **1990**, *112*, 426.

(23) Sáez, M.; Abuin, E. A.; Lissi, E. A. *Langmuir* **1989**, *5*, 942.

(24) The lifetime of $P^{\bullet+}S^-$ was estimated to be ca. 100 μs by analyzing the decay curves at 460 nm observed under O_2 in the 0.15 M SDS solution containing 3×10^{-5} M of NaPS.

(25) Bachmann, P. A.; Walde, P.; Luisi, P. L.; Lang, J. *J. Am. Chem. Soc*. **1990**, *112*, 8200; **1991**, *113*, 8202.

(26) Fendler, J. H. *Membrane Mimetic Chemistry*; Wiley Inter-science: New York, 1982; pp 55−59.

(27) Brunner-Popela, J.; Mittelbach, R.; Strey, R.; Schubert, K.-V.; Kaler, E. W.; Glatter, O. *J. Chem. Phys*. **1999**, *110*, 10623.

(28) Maitra, A.; Mathew, C.; Varshney, M. *J. Phys. Chem*. **1990**, *94*, 5290.

(29) Nazário, L. M. M.; Hatton, T. A.; Crespo, P. S. G. *Langmuir* **1996**, *12*, 6326.

(30) Hait, S. K.; Moulik, S. P.; Rodgers, M. P.; Burke, S. E.; Palepu, R. *J. Phys. Chem. B* **2001**, *105*, 7145.